

Thermal lag and decrement factor of constructive component reinforced mortar channels filled with soil–cement–sa...

Fernando Chinas


Indoor and Built Environment

Cite this paper

Downloaded from [Academia.edu](#) 

[Get the citation in MLA, APA, or Chicago styles](#)

Related papers

[Download a PDF Pack](#) of the best related papers 



[Biocomposite tepexil cement reinforced with fibers of Agave angustifolia Haw as a light mort...](#)

Andy Olivera, Fernando Chinas

[Envelope design for thermal comfort and reduced energy consumption in residential buildings](#)

Saleh Al-Saadi

[Development and Characterization of Gypsum-Based Binder](#)

Faris Matalkah, Anagi M Balachandra

Thermal lag and decrement factor of constructive component reinforced mortar channels filled with soil–cement–sawdust

Rafael Alavéz-Ramírez¹, Fernando Chiñas-Castillo²,
Valentín Juventino Morales-Domínguez¹,
Margarito Ortiz-Guzmán¹, José Luis Caballero-Montes¹
and Magdalena Caballero-Caballero¹

Abstract

In the last years, people has become aware of energy saving and thermal comfort requirements for home buildings in hot and cold seasons. In the present study, hybrid multifunctional constructive components made of a reinforced mortar channel filled with cement–soil–sawdust (CL2MSCAL) were evaluated to experimentally determine their thermal performance (thermal conductivity, thermal time lag and decrement factor). The experimental analysis performed in this study was based on dynamic climatology. Measurements of components surface temperature were conducted to determine temperature damping and temperature wave lag. Monthly average temperature and direct solar radiation data of the site was considered. Measurements of real-scale constructive components were conducted on a fully equipped thermal conductive system and thermal chambers (test cells) built for this purpose. Results are compared to concrete components (CCL) that account for approximately 71.6% of the houses built in Mexico and 43.2% in Oaxaca and reinforced mortar (CML) used as prefabricated housing systems. Best results were found for component CL2MSCAL that has a thermal conductivity of $0.81 \text{ W}\cdot\text{m}^{-1}\cdot\text{K}^{-1}$, a thermal damping of 81.5% (decrement factor of 0.166) and time lag of 7:37 h compared to CCL that present a time lag of 1 h and decrement factor of 0.9. Thus, it is concluded that CL2MSCAL roofing channel components are an alternative for energy saving and thermal comfort.

Keywords

Thermal comfort, Decrement factor, Thermal lag, Soil mixture, Concrete mortar

Accepted: 9 October 2016

Introduction

In the last years, people has become aware of energy saving and comfort requirements for home buildings. Even though at present, construction systems are lighter, they do not have adequate thermal properties to reduce temperature waves from outside. This happens frequently in low-income housing where, generally speaking, adequate materials are not considered as a function of the climatic context to get thermal comfort and energy saving conditions for the user's benefit. For extreme climates with important thermal oscillations

¹Instituto Politécnico Nacional, Research Center for Interdisciplinary Regional Integral Development, Oaxaca, México

²Instituto Tecnológico de Oaxaca, Department of Mechanical Engineering, Oaxaca, México

Corresponding author:

Fernando Chiñas-Castillo, Instituto Tecnológico de Oaxaca, Department of Mechanical Engineering, Calz. Tecnológico No. 125, Oaxaca, Oax. C.P. 68030, México.
Email: fernandochinas@gmail.com

during the day and night, thermal inertia is a necessary thermophysical property since materials have heat storage capacity and release to the inside when temperatures decrease. Thermophysical properties in construction and building materials are an important factor to minimize heat transfer by conduction and radiation and gain energy saving and finally, thermal comfort. In this sense, thermal inertia is a thermophysical property that represents the ability of a material to conduct and store heat and is related to thermal conductivity and volumetric heat capacity while heat transfer in buildings is related to how fast or slow inner temperature reaches outer temperature. The main factors to evaluate thermal inertia are thermal admittance, thermal transmittance, diffusivity, effusivity, heat capacity and time lag and decrement factor. These parameters let us understand the scientific analogy of thermal inertia in building envelopes.

Thermal diffusivity, $\alpha = \lambda / (\rho \cdot C_p)$ $\text{m}^2 \cdot \text{s}^{-1}$, combines the three primary parameters that affect thermal performance of a material, density, ρ ($\text{kg} \cdot \text{m}^{-3}$), specific heat capacity, C_p ($\text{J} \cdot \text{kg}^{-1} \cdot \text{K}^{-1}$) and thermal conductivity, λ ($\text{W} \cdot \text{m}^{-1} \cdot \text{K}^{-1}$). The depth that the daily changes in temperature reach within the material will depend on thermal diffusivity. Thus, materials with higher thermal diffusivity values can be more effective for cyclic heat storage at greater depth than materials with lower values. For example, Maalouf et al.¹ show that hemp concrete has a lower diffusivity than cellular concrete, earth block, solid brick and concrete. The thermal effusivity, β , ($\text{J} \cdot \text{m}^{-2} \cdot \text{K}^{-1} \cdot \text{s}^{-0.5}$), is used to represent the capacity of a material to absorb and release heat. This relationship is also known as the 'thermal inertia' by some authors.² Materials with high thermal effusivity will more readily dissipate heat from their surface and will have a high storage capacity; however, at a surface of a roof/wall, convection and radiation dominate the amount of heat transfer. Both, diffusivity and effusivity methods define the thermal response of a material during the transient period of heat transfer and are typically evaluated through thermal conductivity measurements (under steady-state conditions) and determined by analytical relationships.³ The effective heat capacity is another important parameter that describes the real capacity of a building element to accumulate heat, and recently, Faye et al.⁴ have proposed its experimental determination using the quadrupole method. This analysis starts from an analytical model based on the thermal quadrupole method, and boundary conditions are inputs. In this method, a transmission matrix binds the heat flow and temperature variations on one side of the specimen to those on the other side. Then the specimen is experimentally placed in a climatic chamber under sinusoidal boundary conditions. The thermal properties of the specimen are not

required. This specimen can be heterogeneous and symmetrical. Measurements of temperatures and fluxes are inputs of the analytical model, and the calculation is performed.⁴ Further details on the quadrupole method can be found in Maillet et al.⁵ Transmittance method (also known as U -value) is commonly calculated experimentally via hot-box testing procedure, and the U -value is determined under steady-state conditions also. Admittance method is limited because it uses a simplified treatment of loads.⁶ The key parameter in this method is the thermal admittance, Y ($\text{W} \cdot \text{m}^{-2} \cdot \text{K}^{-1}$), that determines the response of the internal surface to heat. It measures how easy the energy will pass through the internal surface of the constructive element per degree of temperature difference to the room average temperature typically based on a 24-h heat flow sinusoidal cycling. However, no matter how well the U -value is characterized, it will only provide an interpretation of the steady state heat flow through a structure using the basic relationship $Q = U \times A \times \Delta\theta$, where Q is heat flow (W), A is area of wall/roof through which the heat is flowing (m^2) and $\Delta\theta$ is the temperature difference between the two sides of the structure. However in real world, there is rarely a time where there is true steady state. Despite its deficiencies, the benefits of the simplification still holds good even today.

Fatiha et al.⁷ consider that buildings must be designed to have high thermal inertia to obtain a comfortable room temperature, but thermal inertia depends not only from time interval and decrement factor but it is also related to a complex interaction of material density, specific heat capacity and thermal conductivity.⁸ In the past, Orasa and Carpentier⁹ proposed a passive method of energy saving based on thermal inertia in buildings. However, it is still a controversial issue to consider thermal inertia as a determinant parameter in the design stage.¹⁰ At present, methods based on dynamic thermal characteristics as design criteria of buildings are taking much attention because they brings the possibility of increasing thermal efficiency of a construction system.^{11,12} It is considered that thermal conductivity on its own is not and cannot be the only reliable indicator of energy saving and do not represent with high accuracy the dynamic thermal behaviour of a system.¹³ The last two additional and very important factors mentioned above are time lag and decrement factor (sometimes called thermal damping or amplitude reduction), both of which are influenced by thermophysical properties of material, thickness and orientation.¹⁴ For humans, roofing provides the main protection against direct solar radiation, thus is also important to properly select its material with good thermal properties to improve the comfort in the inner ambient. An exposed roof absorbs solar radiation

during the day and its surface temperature rises. Then it re-radiates the absorbed heat at night and its surface temperature drops. Vecchia¹⁵ indicates that exterior building walls are seldom in steady-state conditions and air temperatures inside a house follow the same daily cycle pattern as outdoor surface temperatures determined by the combination effects of sun radiation and ambient air temperature in a transient regime of periodic type. Under these conditions, the response of walls to temperature changes is a function of both thermal resistance and heat storage capacity.

Soil, one of the main materials in this study, has been used since 10,000 years ago when men learned how to build their own houses. It is estimated that more than a third part of the people live in a house built with soil. In soil construction worldwide, there exist 12 recognized methods of construction.¹⁶ Soil, as a construction building material, has shown advantages in acoustic and thermal damping, besides, raw material and the fabrication process is environmentally friendly; however, construction regulations do not recommend it because of the low structural stability, water and mechanical resistance and as such, these materials have been almost substituted by modern building materials that do not share the same advantages that soil materials have (i.e. thermal inertia for thermal comfort).

Studies on thermal damping for building components used in Mexico are just a few, mainly because construction regulation does not force local builders to respect minimum values of thermal resistance in constructing materials. However, worldwide, there are some efforts at research level directed to determine thermophysical properties of construction materials. Krüger et al.¹⁷ evaluated thermophysical properties of a composite panel of cement and wood determining heat flow and temperatures inside a small experimental cells 1 m³ during winter and summer, following the work from Bederina et al.¹⁸ Morris et al.¹⁹ carried out experimental work to evaluate the benefits of insulated and non-insulated roofing, constructing two identical chambers of 4 m × 4 m × 3 m with conventional materials for the enclosure. Results indicate that insulated roofing reduces the inside temperature during the day up to 8°C. Ouldboukhitine et al.²⁰ took into account the effects of solar radiation in green roofs of experimental cells by a thermodynamic model based on energy balance, characterizing their thermophysical properties. The results indicate that vegetation in roofing can improve not only thermal comfort but also energy performance of a construction building. Tibério-Cardoso et al.²¹ studied the thermophysical properties of polyurethane hard foam panels extracted from castor plant, considered to be environmentally friendly, in experimental cells of 2.20 m × 2.70 m showing that this material can be used as thermal insulation in roofing systems.

Gameros-Gonzalez²² studied the thermal performance of passive air conditioning made from Polyethylene terephthalate (PET) bottles filled with water at different levels. The author reported that the more water in the bottles the higher the efficiencies registered.

The thermal performance of roofing materials have been evaluated on real-scale buildings in recent years. Roels and Deurinck²³ studied the thermal emissivity of five well-insulated roofs in a real-scale test building with thermocouples and heat fluxes sensors. Temperature measurements on a full-scale test building showing that hemp-lime biocomposite provides a significant amount of oscillation attenuation in the external environment for thermal comfort during summer within the building were reported by Shea et al.²⁴ Vecchia and Castañeda^{25,26} performed experimental thermal studies using a dynamic climate methodology on a prototype house made of bajareque, clay, asbestos-cement and galvanized steel with polystyrene; the resulting bajareque, which is an excellent option in thermal insulation of properties for low-income family houses in hot climates. Singh et al.²⁷ generated specific equations for the prediction of maximum and minimum temperatures inside two vernacular houses from one year collected data of roof surface temperatures, relative humidity and illumination level in hot and cold climate. Roma Jr. et al.,²⁸ using a dynamic climate methodology, showed that thermal performance, amplitude reduction and delay of sisal and eucalyptus roofing tiles is better than asbestos-cement; being fibre type, the content is the main variable to improve their mechanical properties. Temperature fluctuations of green roof and a sod roof with a bituminous membrane roof and a steel sheet roof were studied by Teemusk and Mander,²⁹ reporting no increase in temperature of planted roofs during summer, higher amplitude reduction and cooled more while in winter; temperatures were higher than the surfaces of conventional roofs.

More recently, Alavéz-Ramírez et al.^{30,31} measured the thermal conductivity of ferrocement roofing channels filled with coconut fibre and studied their thermal lag and decrement factor behaviour on a real-scale prototype house. Results indicate that these constructive components have a low thermal conductivity, thermal lag of about 3½ h and 40% thermal damping.

Now in this research work, the same authors presents an experimental study of thermal time lag and decrement factor on roofing constructive components made of reinforced mortar channels filled with soil-cement-sawdust (CL2MSCAL) for houses located in Oaxaca City, Oaxaca, Mexico during cold season. The construction component design is modular and pre-manufactured to be used by one-level low-income houses. Much has been said about the advantages of soil's properties such as its thermal conductivity and thermal mass, but at present

there are no similar experimental studies on large building components reported in the literature. It was decided to carry out a thermal monitoring on real-scale roofing constructive components ($1\text{ m} \times 1\text{ m} = 1\text{ m}^2$) in full-scale test cells, planned to ensure equivalence to a real situation for data acquisition, in order to measure temperature data coming from the heat transmission mechanisms present (radiation, conduction and convection). The only variation involves the different types of roof constructive component. The experimental analysis was based on dynamic climatology and measurements of roof surface temperatures were conducted to determine temperature damping and temperature wave lag. Monthly average temperature and direct solar radiation data of the site was considered. Thus, it is believed that the methodology applied in the present paper is more realistic. Results are compared to concrete components (CCL) that account for approximately 71.6% of the houses built in Mexico and 43.2% in Oaxaca during 2010 and reinforced mortar (CML) used as prefabricated housing systems in Oaxaca.^{32,33} Thermal conductivity measurements were also performed using a fully equipped thermal conductive system for real-scale constructive components of 1 m^2 .³⁰ All data set are not included in the paper, but it can be available upon request.

This proposal emerges as an improved version of soil combined with pre-manufactured elements of reinforced concrete to form a construction component with adequate thermal properties and thermal inertia to guarantee safety and comfort to houses built taking advantage of a cooling and heating passive system. In this sense, a passive system will be efficient as far as maximum and minimum temperatures may be lower than inside temperatures or higher (because of thermal inertia) than outside temperatures when they are too low. The higher these gradients become the greater the heating or cooling efficiencies become. In the components studied, reinforced mortar (which has a very low thermal capacity), whose properties have already been determined under several working conditions, i.e. traction load, flexion, compression, shear, fatigue, elastic modulus, specific surface stress and cracking characteristics of structures built with this material, provide mechanical resistance and soil-cement-sawdust filler acts as a thermal damping material.^{34,35}

Experimental methodology

Oaxaca City is the capital of the Mexican state of the same name (Oaxaca) and is located in the southeast part of the Mexican Republic at geographic coordinates of $17^{\circ}04'04''\text{N}$ latitude and $96^{\circ}43'12''\text{W}$ longitude and 1550 m altitude above sea level with a mild climate.³⁶ Summer is tropical semi-hot sub-humid and oriental low lands present a temperature that ranges

Table 1. Average climatic data of Oaxaca City.

	Annual	January
Maximum temperature ($^{\circ}\text{C}$)	30.4	28.8
Minimum temperature ($^{\circ}\text{C}$)	13.6	9.5
Mean temperature ($^{\circ}\text{C}$)	22	19.1
Thermal oscillation ($^{\circ}\text{C}$)	16.8	19.3
Wind mean speed ($\text{m}\cdot\text{s}^{-1}$)	1.8	1.7
Total radiation ($\text{kWh}\cdot\text{m}^{-2}$)	682.5	672
Relative humidity (%)	65.6	58

from 9°C to 34°C during the daytime. This city exhibits a moderate relative humidity with summer rain as classified by Köppen.³⁷ Wind moves from north to south and presents intense solar radiation in clean days. A climatic analysis of weather data from Oaxaca City was carried out in order to know the variables that influence the dynamic thermal behaviour. For that effect, mean monthly temperature data registered during a 30 years' time period (1980–2010) was provided by Servicio Meteorológico Nacional (Mexico's national weather organization), and Table 1 summarizes average local climatic data from the last decade.³⁸ Temperatures were taken into account as representative of winter and summer season. From these data, maximum, minimum and average monthly values were obtained. There exist an annual thermal oscillation of 16.8°C , and García³⁹ reported that during January this value could reach 19.3°C , which is more than 14°C above the annual average.

Koenigsberger⁴⁰ suggests that when daily oscillations are above 10°C , thermal inertia strategies should be considered to induce thermal damping. Mean temperature data were used to determine the neutral temperature and comfort zone of the locality using a model from Aulliciem equation⁴¹ according to equations (1) and (2).

$$T_n = 17.6 + 0.31(T_m) \quad (1)$$

$$T_{cz} = T_n \pm 2.5 \quad (2)$$

where T_n = neutral temperature ($^{\circ}\text{C}$), T_m = mean temperature ($^{\circ}\text{C}$) and T_{cz} = comfort zone temperature ($^{\circ}\text{C}$). In this way, it was determined that the thermal comfort zone for January, the month with the highest thermal oscillation, was 21.0°C and 26.0°C .

Properties of materials used in constructive components

Reinforced mortar is a construction material composed of concrete reinforced with various layers of steel wire mesh electro-welded or hexagonal, distributed

uniformly through a transversal section. Normally, a mortar rich of cement, sand and water is used. This material is thin (10–35 mm width) and with high resistance and flexibility besides of being a low-cost material.

The cement used for the reinforced mortar channels was Portland type 1 (Cooperative La Cruz Azul S.C.L. in Mexico) that fulfils all requirements of ASTM C-150-89 standard.⁴² Natural sand was clean and free from organic substances and sieved with sieve #8 (2.38) ASTM with an average grain size of 0.7 ± 0.145 mm. Water was taken from the main distribution line in the region to prepare the mixture. Table 2 summarizes the mechanical properties of mortar used in this study to make the channels for roof and walls.⁴³

Properties and granulometry of soil

Soil was selected on the basis of a Unified System of Soil Classification. The soil was collected from surrounding suburbs of Oaxaca City: (1) Trinidad de Viguera, Oaxaca, located at geographical coordinates $17^{\circ}7'50''$ N latitude and $96^{\circ}45'1''$ W longitude and (2) Santa Cruz Xoxocotlán, Oaxaca, located at geographical coordinates $17^{\circ}1'53''$ N latitude and $96^{\circ}43'56''$ W longitude, and classified according to granulometry

tests, consistency limits and plasticity chart.⁴⁷ This selection was done considering the material texture from sandy-clayey soil for walls and clayey soil for roof. The required quantity of subsoil was mechanically dug and transported to the experimental site. This soil bank localization is shown in Figure 1. There, a soil sampling by quartering was used to get a representative sample of the collected soil zone, according to the Mexican Official Standard NOM-AA-61.⁴⁸

A granulometric analysis of sieved soil was carried out according to ASTM D422 standard.⁴⁹ This test determined the percentage of sized particles in the soil, expressing the quantity which passed through the meshes in the used sieves, down to the mesh 200. Volumetric dry weight for the two soils selected was determined before the granulometry test. This was measured dividing the corrected weight by the Tara volume. The specific weight of soil from Santa Cruz Xoxocotlán and Trinidad de Viguera were $1318 \text{ kg}\cdot\text{m}^{-3}$ and $1168 \text{ kg}\cdot\text{m}^{-3}$, respectively.

Specific weight and ASSHTO test for optimum humidity

Maximum specific weight and optimum humidity of selected soils used in this work was determined based on the Proctor compaction test (ASSHTO T99 standard)⁵⁰ to know the amount of water needed and, a graph of compaction for the two selected soils was formed. This graph was used to prepare the mortar for (a) soil + sawdust + cement for roof slabs and (b) soil + cement for walls. The soils were compacted into the mould of a manual machine to a certain amount of equal layers, each receiving a number of blows from a standard weighted hammer at a specified height. This process was then repeated for various moisture contents and the dry densities were determined. After that, the samples were weighted and dried in an electric oven at 105°C for 72 h until a constant weight was

Table 2. Properties of mortar.

Property	Measured value	International standard
Cement: sand: water	1:3:0.67	–
Compression strength of cylinders	25.29 MPa	ASTM C39/C39M-03 ⁴⁴
Compression strength of cubes	23.03 MPa	ASTM C109/C109M-02 ⁴⁵
Elasticity modulus	16.3 GPa	ASTM C469-02 ⁴⁶
Poisson ratio	0.11	ASTM C469-02 ⁴⁶

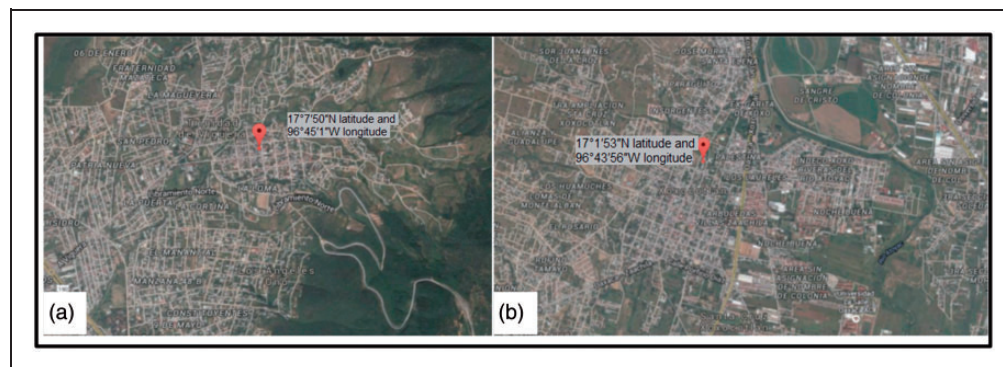


Figure 1. Geographical location of soil banks in Oaxaca City and its surrounding suburbs.

attained. The graphical relationship of the specific weight to water content was then plotted to establish the compaction curve observed in the results. Optimum humidity was calculated using equation (3)

$$A = w_m \frac{w_2 - w_1}{100 + w_1} \quad (3)$$

where A = volume of water to add (ml), w_m = weight of sample for initial moisture (gr), w_1 = initial moisture of the sample (%) and w_2 = optimum humidity (%).

After soil was conditioned, what followed next was making the constructive channels and preparing the channels' fillers proposed in this study, considering the optimum water content that resulted from ASSHTO test and specific weight. For soil stabilization and channel filled with reinforced mortar for walls, it was decided to use a sandy clayey soil + 10% cement (SC), a ratio suggested by several authors.^{51,52} On the other hand, a low specific weight for channels fillings was desirable in slabs. With these in mind, four mixtures were prepared with cement, sawdust wood and soil (CAS), as indicated in Table 3.

Compressive test of fillers for roof channels

The axial compression test was carried out to evaluate the strength and durability of mixtures for roof channels in accordance with Mexican standard norm NMX-C-037-ONNCEE⁵³ at 32°C with $28 \pm 2\%$ relative humidity on five replicate samples for each test. The apparatus used for axial compression tests was a Geotest Instrument Corp series S5830 Multiloader with an end scale of 50 kN.

Fabrication of reinforced mortar channels

Details of dimensions, expressed in metres, and configuration of constructive components under study as 3D rendered images indicating the materials are shown in Table 4.

Specimens under study were made as follows: Roof component CL2MSCL was formed by two reinforced concrete channels of 50 cm wide filled with casted soil + 10% cement and a slab of reinforced concrete + half red clay brick + mortar slurry of cement-sand as roof-finishing to prevent water filtrations. Roof component CL2MSCAL was formed by two reinforced concrete channels of 50 cm wide filled with casted soil + 10% cement + sawdust and a slab of reinforced concrete + half red clay brick + mortar slurry of cement-sand as roof-finishing to prevent water filtrations. Thermal lag and decrement factor of these two constructive components was measured and compared to the rest of the specimens prepared: wall component CMMSC was formed by two reinforced concrete channels of 50 cm wide filled with casted soil + 10% cement. Component CLMSCA was formed by two reinforced concrete channels of 50 cm wide filled with casted soil + 10% cement + sawdust. Component CL2MAL was formed by two reinforced concrete channels of 50 cm, a slab of reinforced concrete + half red clay brick + mortar slurry of cement-sand as roof-finishing to prevent water filtration. Component (CCL) was formed by a concrete slab + half red clay brick + mortar slurry of cement-sand. Component (CML) was formed by reinforced mortar + half red clay brick + mortar slurry of cement-sand.

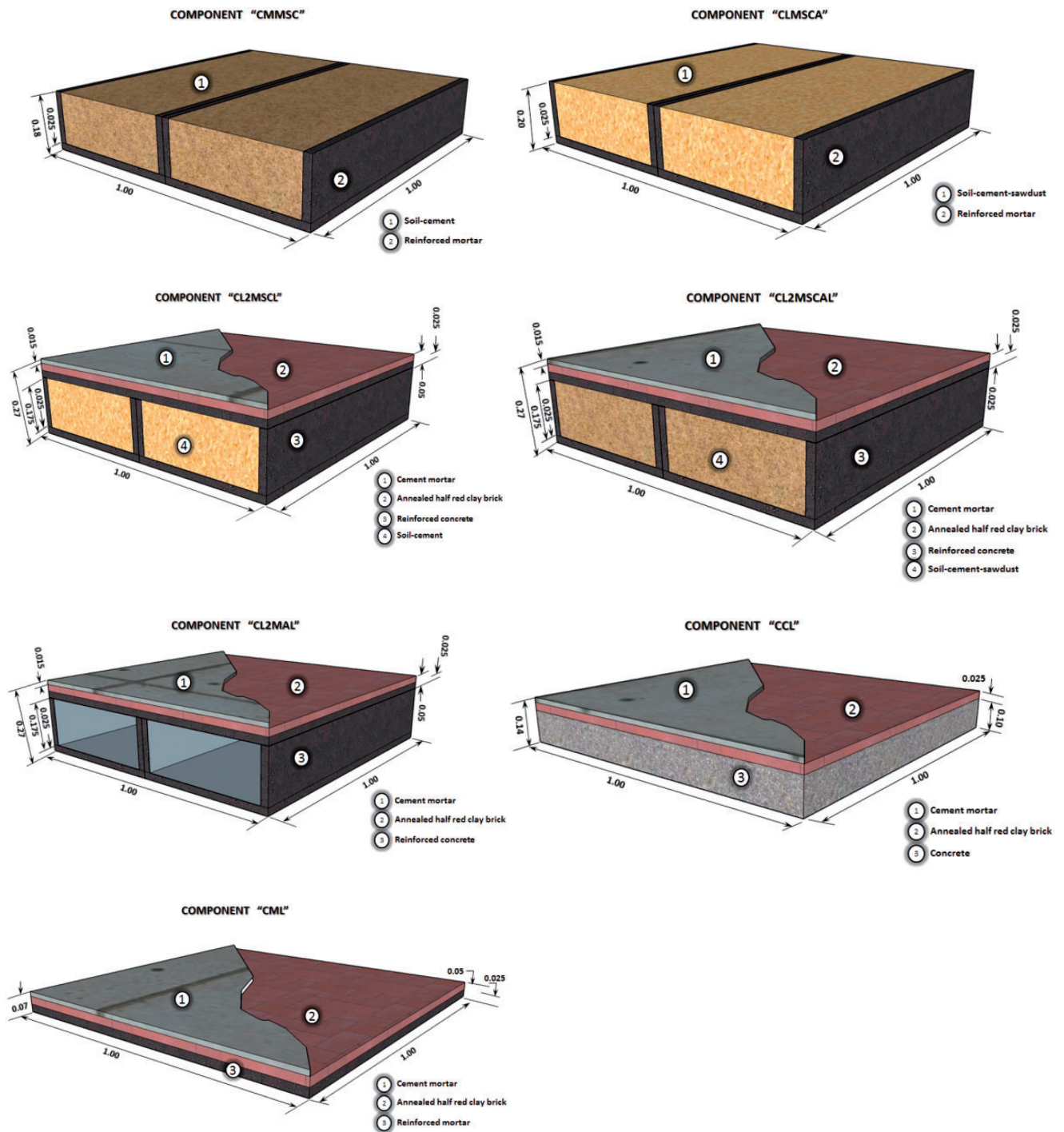
A pine wood formwork was made before the fabrication of reinforced mortar channels. This was formed by three panels: Panel 1 was the walls of the channel, Panel 2 was the peripheral wood of channel for skids of 18 cm and Panel 3 was the inside skids of channels. Figure 2(a) and (b) shows architectural ground plan and cross section from wood formwork, respectively. Figure 2(c) shows the finished wood formwork. A wood preservative was applied at the end on the wood formwork.

The fabrication of channels was formed with an electrowelded mesh size $6 \times 6/8 \times 8$ and chicken-wire mesh $\frac{1}{2}$ opening. Mortar cement-sand was poured over Panel 1 and lateral skids on Panels 2 and 3 (see Figure 2(d)); The mortar matrix for channels was a mixture of

Table 3. Mixture portions for roof slabs (kg).

Sample	Cement (kg)	Sawdust wood (kg)	Soil (kg)	Water (L)	Solids	Humid material	Tara volume (m ³)	Humid specific weight (kg·m ⁻³)	Dry specific weight (kg·m ⁻³)	Humidity (%)
1	0.5	1.2	3	4.5	4.7	4547	2.691	774.1	401.0	93.05
2	1	1.2	3	4.5	5.2	4632	2.6941	805.6	430.2	87.27
3	2	1.2	3	4.8	6.2	4941	2.6941	920.5	513.6	79.21
4	2.5	1.2	3	4.8	6.7	5007	2.6941	945.0	536.6	76.10

Table 4. Dimensions of constructive components under study.



cement: sand: water with a proportion of 1:3:0.67. Reinforced mortar channels were kept in the lab under ambient temperature and covered with a plastic membrane, moisturizing them twice a day. Figure 2(e) shows the finished channel of 0.50 × 1.00 m side and 0.18 m the cant and thickness of 0.025 m.

Fabrication of experimental cells

Seven experimental cells of 1 m³ were made to evaluate the thermophysical properties of constructive components under study. These experimental cells were adapted from Haik,⁵⁴ and a detailed description is shown in Figure 3(a)

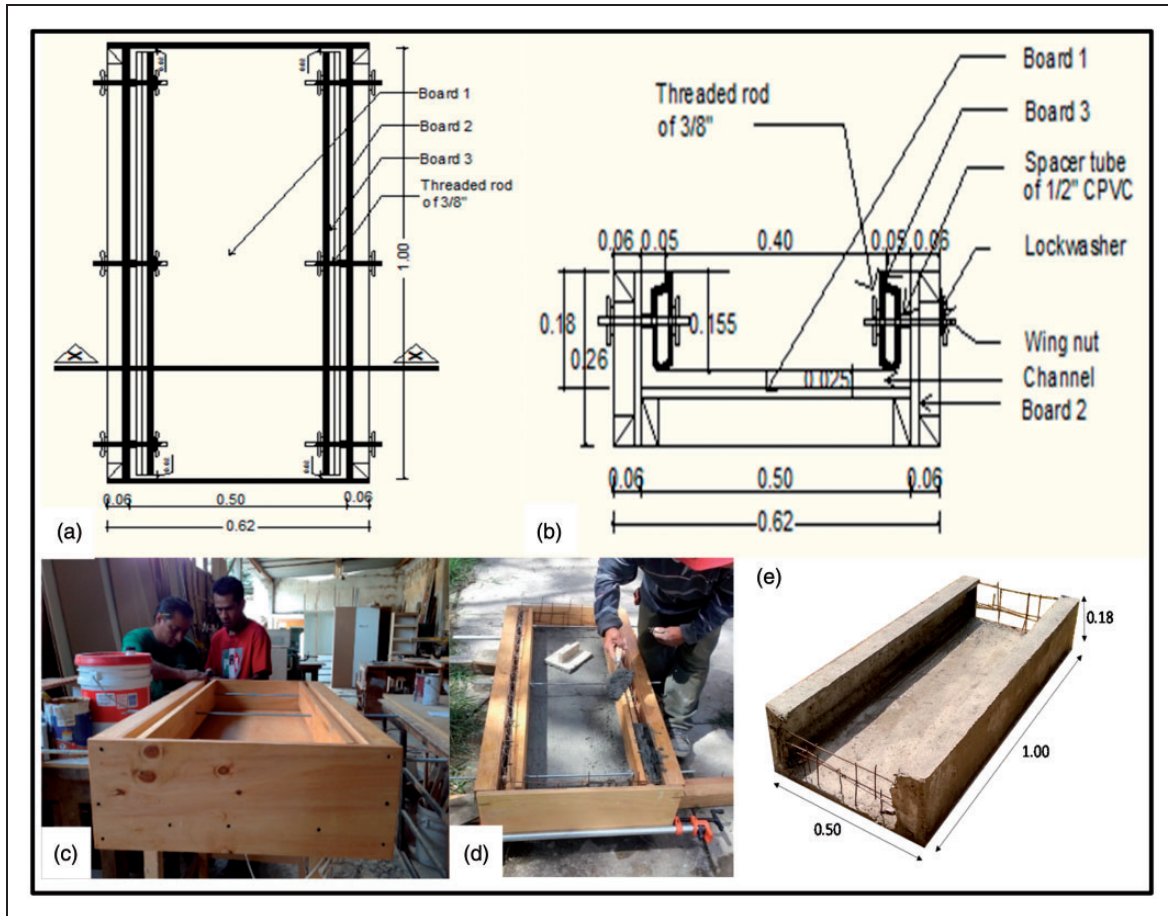


Figure 2. Drawings of formwork and fabrication of reinforced mortar channels: (a) architectural ground plan, (b) cross section and (c)–(e) wood formwork and finished channel.

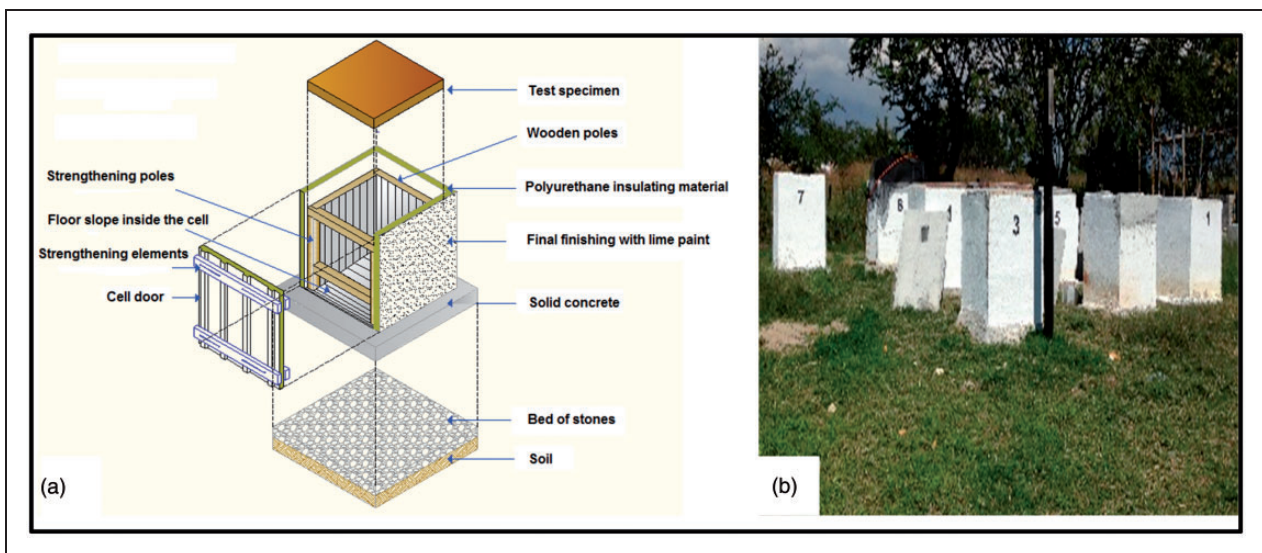


Figure 3. (a) Assembly of experimental cell. (b) Finished experimental cells.

and (b). The construction process of the experimental cells began by preparing the terrain, levelling and compacting (layers of 15 cm) and, after that, a slope preparation of 30 cm of soil for each cell; on that firm ground, a gravel bed was placed in order to avoid soil humidity by capillarity; four poles were supported on a firm concrete and a rigid wood framework was built to sustain the insulating envelope with plates of polyurethane coated with a thin layer of mortar cement: sand and finishing with a limo slurry for sun reflexion. Finally, specimens under study were placed in the experimental cells.

Temperature measurements on constructive components

A period of this study (in this case, the month of highest thermal oscillation) was considered to carry out all the experimental measurements to take into account the thermal mass effect during winter time as an strategy of passive design in roof and walls. Thus, temperature data from normal weather conditions for Oaxaca City for a period of 30 years (1980–2010) were used.³⁸ Its analysis was carried out on a datasheet according to a bioclimatic design methodology.³⁶ The bioclimatic methodology is not included in the paper for the sake of brevity but it can be available upon request.

In thermal time lag and decrement factor or damping determination, only surface temperatures were involved, and these in turn depend on constructive component material thickness and thermal properties. It is important to mention that in this work only the thermophysical properties of the roofing components were considered and not the complete test cell. Thermal time lag is defined as time delay due to the thermal mass. Thermal time lag was determined as

the time difference between maximum temperature on the outside surface of the constructive component under the study and the maximum temperature on the inside surface. A material with thermal lag values as high as 8 or 9 h, could take hours for heat to flow from one side of the envelope to the other, and it has a high thermal mass, for example double-brick or earth walls. The decrement factor is the ratio between the temperature fluctuation on the outer and the inner surface. It is the measure of the damping effect and refers to the amount by which conditions are moderated by an element of a building. Generally, the higher the thermal capacity or the higher the thermal resistance of a material, the stronger is the damping effect. Thus, to reduce overheating, a low decrement factor is required, and a time lag of 6 to 12 h.

Seven experimental cells were used to measure inside and surface temperatures of constructive components and plot the time lag and decrement factor, respectively. Dimensions of experimental cell prototype and hobo location for temperature measurements are shown in Figure 4(a) and (b). A total of seven hobo type data loggers U12 were required. An additional hobo was used for outside temperature and humidity.

A hobo data logger was located 2.5 m high inside a thermal coating to avoid direct solar radiation while providing cross ventilation to record exterior air temperature.

Measurements of surface temperatures in the seven constructive components were taken with a total of 28 sensors type TMC6-HD Smart sensors (-40°C to 100°C) connected to a 12-bit HOB012 data logger system that includes a HOB0ware software and a NIST standard calibration kit and stores 43,000 readings at a sampling speed of 1 s to 18 h. Two sensors

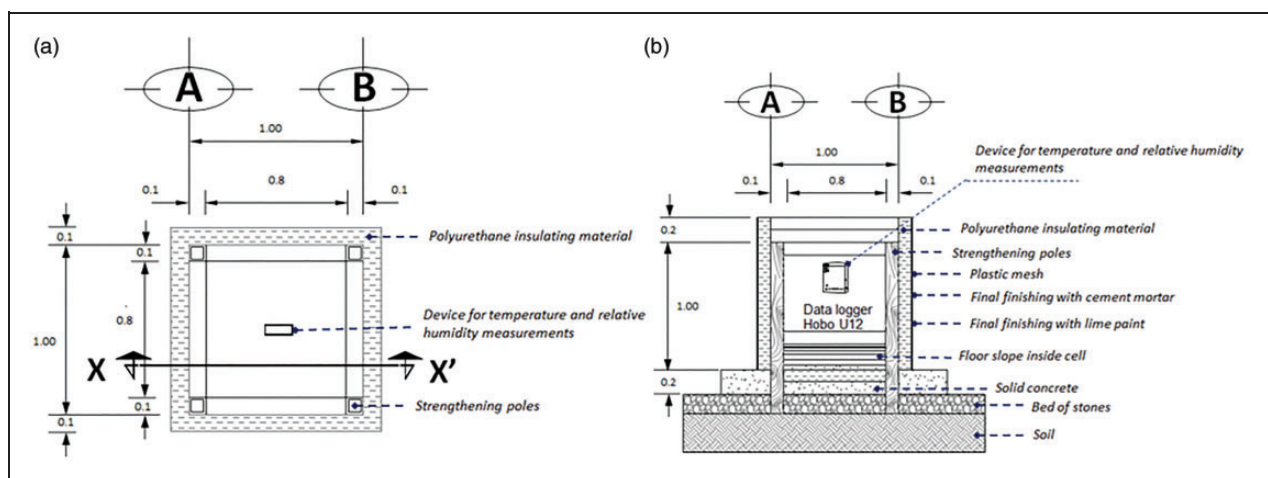


Figure 4. Dimensions of experimental cell: (a) upper view and (b) cross section.

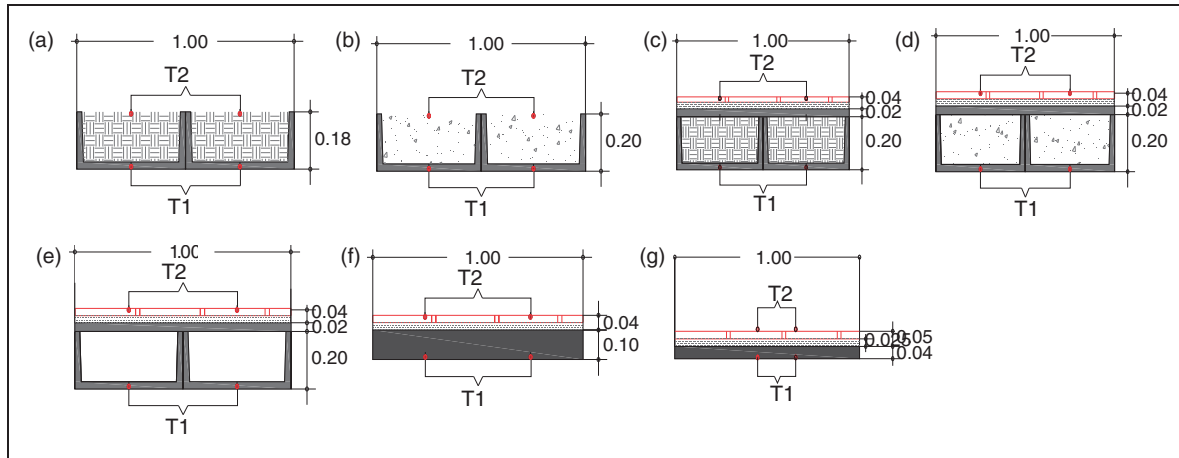


Figure 5. Configurations of constructive components and sensors location: (a) CMMSC, (b) CMMSC, (c) CL2MSCL, (d) CL2MSCAL, (e) CL2MAL, (f) CCL and (g) CML.

were located on inside surface of the component and other two on the outside surface of component, one more sensor was able to measure the external ambient temperature. Figure 5 show configurations of components and sensors' locations.

Thermal conductivity measurements on constructive components

Thermal conductivity measurements of constructive components used in this study were carried out on a hot plate conductivimeter developed by the authors from previous studies.³⁰ In its basics, this apparatus is a box one side open, in which heat is generated by means of an electric heating system. The walls of the box are thermally isolated with a ceramic fibre material. Dimensions of the apparatus and further details can be found in Alavéz-Ramírez et al.³⁰ This is a primary apparatus that uses steady state conduction heat transfer as principle and allows determining thermal conductivity by ASTM C 177⁵⁵ using equation (4):

$$\lambda = q \cdot L / (A \cdot \Delta T) \quad (4)$$

where q is heat flow rate through the specimen in W, λ is the equivalent thermal conductivity of the specimen in $\text{W} \cdot \text{m}^{-1} \cdot \text{K}^{-1}$, ΔT is the temperature difference through the specimen in K, L is the thickness of the specimen in m and A is the area of cross section in m^2 . If the specimen is a compound contains porous or voids where heat can be transferred by convection, radiation and/or conduction, then λ , in equation (4), is the apparent or equivalent thermal conductivity of the constructive component.

Equivalent thermal conductivity was determined mounting each constructive component on the open

side and closing the box completely. A constant heat flow of 100 W was supplied to the component of area 1 m^2 through a controlled power supply and a 500 W stainless steel mica insulated strip heater (large 100 cm \times wide 100 cm) with five holes to be attached to the constructive component. Temperatures were recorded by TC6-J type thermocouples (temperature range 0°C–800°C) and a data acquisition system, four channels HOBO UX120-014 M. Four testing replicates were carried out on each component in this study. More than 100 points in the steady state were taken to calculate the mean temperature registered in every sensor for each component tested. Registered values used to determine the equivalent thermal conductivity of the material tested correspond to the steady state.

Results and discussion

Soil chemical composition and grain size distribution

The selected soils collected were composed of the following: (1) Soil bank from Trinidad de Viguera shows a SiO_2 content of 70.44% and Al_2O_3 content of 13.29% that means this soil can be agglutinated by itself and stabilized with organic and cemented matter like calcium hydroxide, available in cement or lime. This soil can be used for roof slabs combining sawdust and a low percentage of cement for stabilization and relatively low specific weight. (2) Soil bank from Santa Cruz Xoxocotlan shows a lower silica oxide than soil from Trinidad de Viguera. This soil sample presented higher aluminium oxide content (16.04%), and it was selected to be used as filler for wall components combined with 10% cementing material for stabilization.

The chemical characterization of the selected soil samples is essentially composed of:

1. Soil bank from Trinidad de Viguera: SiO₂ (70.44%), Al₂O₃ (13.29%), Fe₂O₃ (4.05%), Fe (4.21%), PXC (5.40%), K₂O (2.81%), Na₂O (0.36%), Mg O

(0.09%), CaO (0.28%), TiO₂ (1.06%), FeO (1.77%), P₂O₅ (<0.06%) and MnO (0.08%).

2. Soil bank from Santa Cruz Xoxocotlan: SiO₂ (51.57%), Al₂O₃ (16.04%), Fe₂O₃ (9.07%), Fe (7.16%), PXC (7.81%), K₂O (1.80%), Na₂O (1.76%), Mg O (1.61%), CaO (3.82%), TiO₂ (2.85%), FeO (1.05%), P₂O₅ (<1.39%) and MnO (0.16%).

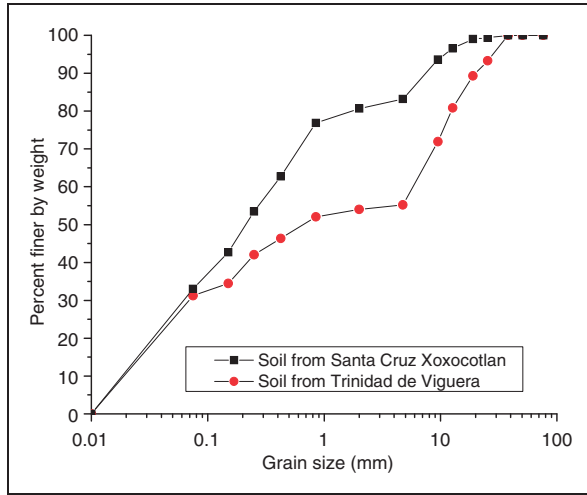


Figure 6. Grain size distribution of soils from Trinidad de Viguera and Santa Cruz Xoxocotlan.

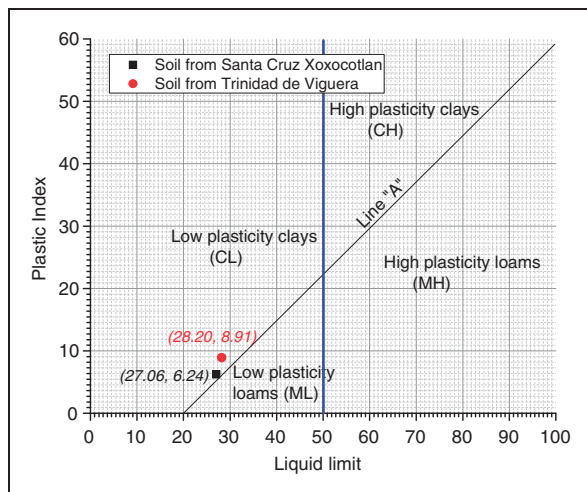


Figure 7. Unified Soil Classification System (USCS) chart for soils from Trinidad de Viguera and Santa Cruz Xoxocotlan.

The grain size distribution and the Atterberg limits of a soil are required for classification by the AASHTO System. The selected soils can be classified as follows: (1) bank from Trinidad de Viguera with 57% fines is classified as soil type CL or low plasticity clayey sand soil type with liquid limit LL 28.20%, plastic limit PL 19.29%, plastic index PI 8.91%, lineal contraction LC 3.51%, and (2) bank from Santa Cruz Xoxocotlan with 40% fines is classified as soil type CL or low plasticity clayey sand soil type with liquid limit LL 27.06%, plastic limit PL 20.82%, plastic index PI 6.24%, lineal contraction LC 2.41%. Figures 6 and 7 show a grain size distribution curve and Unified Soil Classification System (USCS) graph of the selected soils used in this study.

AASHTO optimum humidity

After the AASHTO test was finished, it was concluded from its results that the specific weight and optimum humidity was (1) Trinidad de Viguera (1838 kg·m⁻³ and 14%) and (2) Santa Cruz Xoxocotlan (1745 kg·m⁻³ and 18.5%).

Volumetric weight and axial compression of constructive components' fillers

Mixture 1 in Table 3 was the sample that shows the lowest humid volumetric weight (774.1 kg·m⁻³); however, its consistency was inadequate, and for this reason, mixture 4 was used since it had a volumetric weight of 945 kg·m⁻³ and better consistency. Results from Table 5 show that humid volumetric weight from mixtures soil-cement in walls was 1853 kg·m⁻³ for 1 kg of cement per every 10 kg soil. Table 5 shows quantities per m³ for mixture used as filler in walls constructive channels.

Results from Table 6 show that mixture CAS4 has the highest average 28 days compressive strength.

Table 5. Mixture portions for walls (kg).

Sample	Cement (kg)	Soil (kg)	Water (L)	Solids weight	Weight of humid materials	Tara volume (m ³)	Humid volumetric weight (kg·m ⁻³)	Dry volumetric weight (kg·m ⁻³)	Humidity (%)
Soil-cement	1	10	4	15	4,988	2.691	1,853.6	1,353.6	36.94

Mixture CAS4 do not present a compressive strength high enough to be used as structural loading; however, it has mechanical features of an insulating material and adequate consistency to be used in roof slabs.

Monthly temperature analysis

The coldest month of the year is the month of January for what the thermal analysis of the constructive components under study was carried out in this paper. Figure 8 shows these lowest temperatures for Oaxaca City.

Figure 9 shows temperature measurements registered inside the experimental cells during January. Measurements shown are from 20 to 23 January 2015 (the most stable temperatures in that month).

Results from Figure 10 show values of outside surface temperature while Figure 11 shows values of inside surface temperature in components tested during 20 to 23 January. Thermal amplitude results of the

constructive components tested are as follows: (1) CL2MSCL (5.71) < (2) CL2MSCAL (5.72) < (3) CLMSCA (8.38) (4) CMMSC (8.56) < (5) CL2MAL (11.01) < (6) CCL (14.17) < (7) CML (16.44), where roof slab component specimen formed by two plates of reinforced mortar and soil-cement as filler (CL2MSCL) and roof slab component with two plates of reinforced mortar plus soil-cement and sawdust as filling material (CL2MSCAL) got the best thermal amplitudes. The average amplitude recorded outside the cells was 21.83°C and as such, it may well be recommended the use of thermal mass materials.

Decrement factor and thermal lag of constructive components

Decrement factor (sometimes called thermal damping) of constructive components under study was determined as the ratio between maximum temperature difference of inside surface and maximum temperature difference outside surface. Effectiveness of constructive component was calculated through its decrement factor using equation (5):

$$\mu = \Delta T_{in} / \Delta T_{ov\tau} \tag{5}$$

where μ is the decrement factor of component, ΔT_{in} is the inside maximum surface temperature difference of the day and $\Delta T_{ov\tau}$ is the outside maximum surface temperature difference of the day.

Table 6. Axial compressive strength in slabs.

Mixture	Mean compressive strength (kg.cm ⁻²)
CAS 1	0
CAS 2	0.361
CAS 3	0.372
CAS 4	0.759

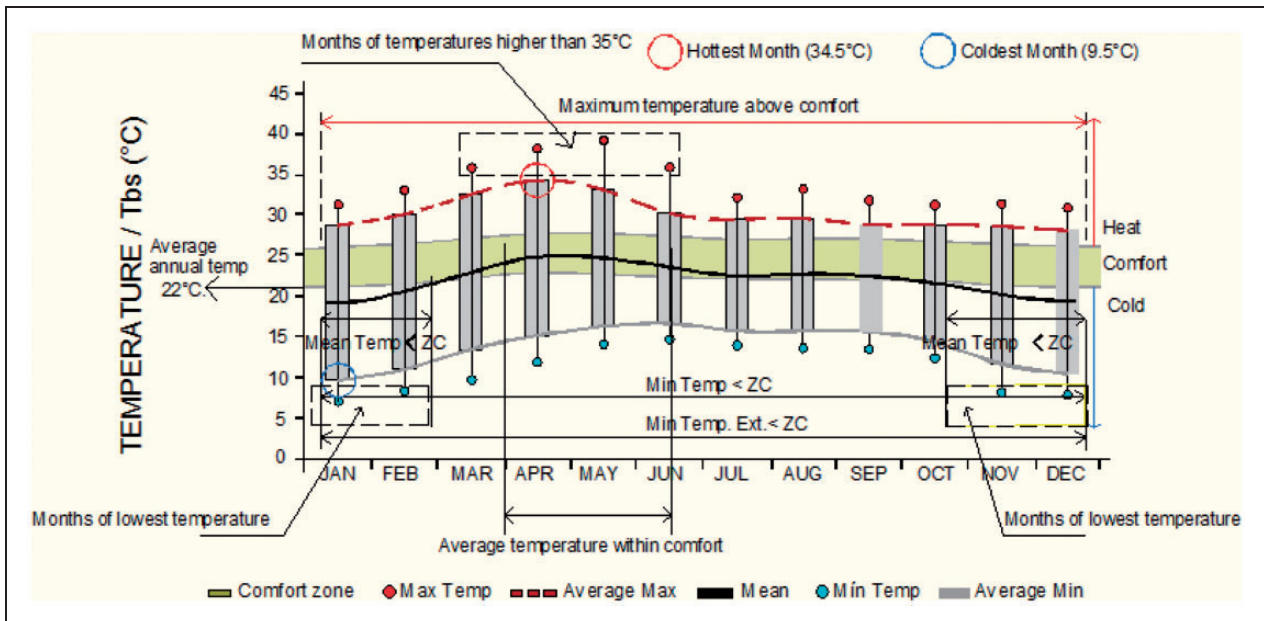


Figure 8. Monthly temperatures for Oaxaca city.

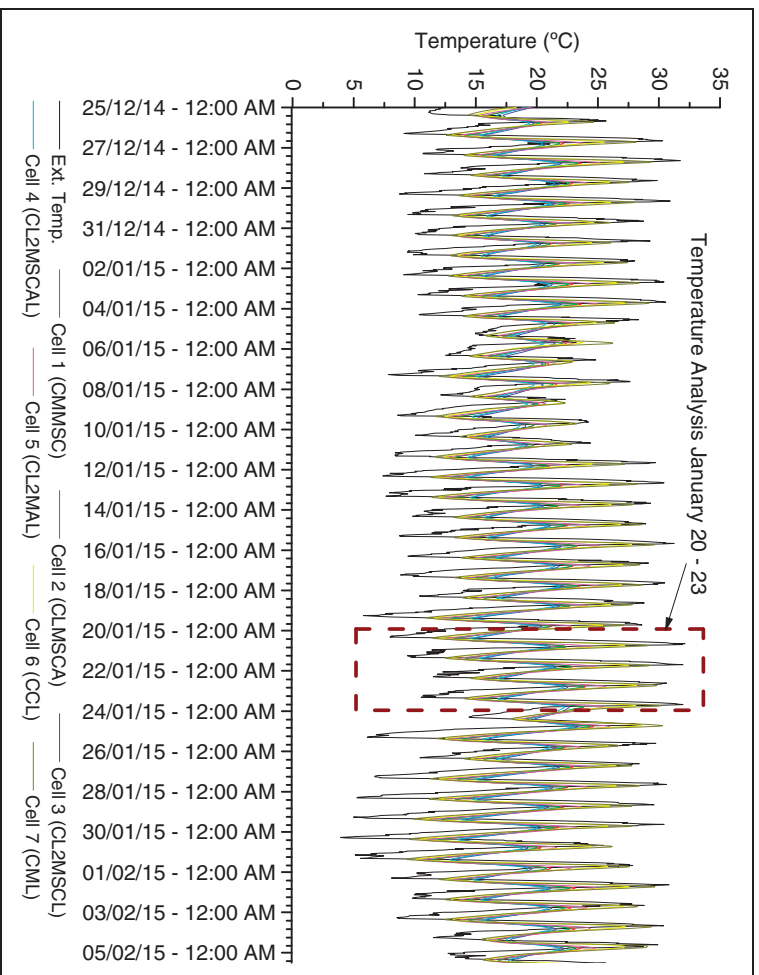


Figure 9. Ambient temperatures internal + external (20 to 23 January).

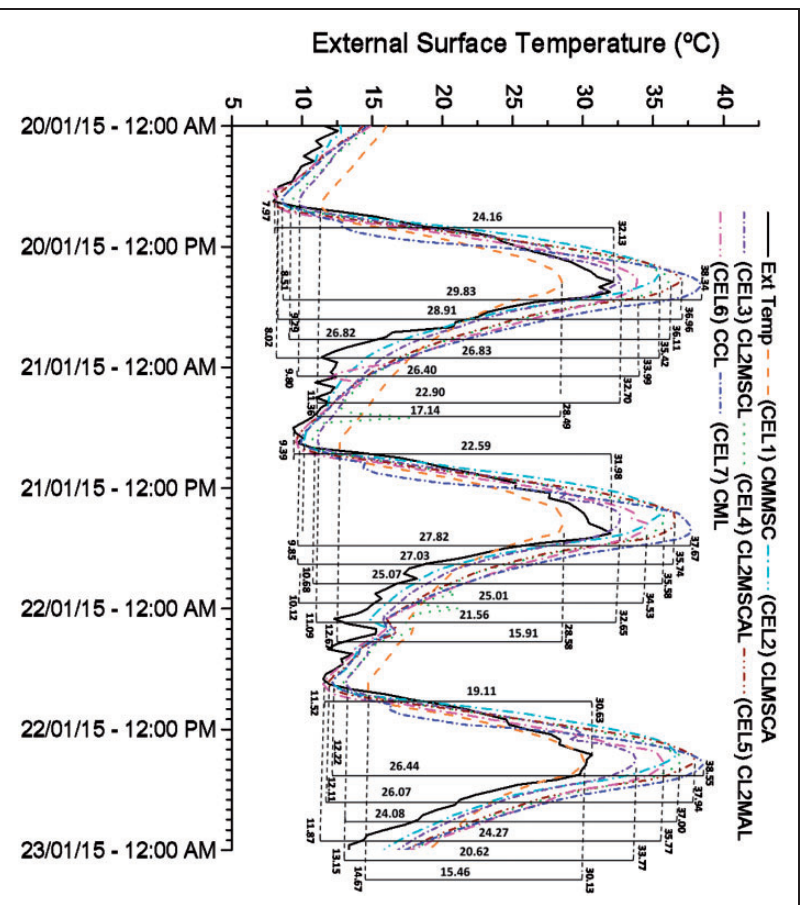


Figure 10. Outside surface temperatures of constructive components.

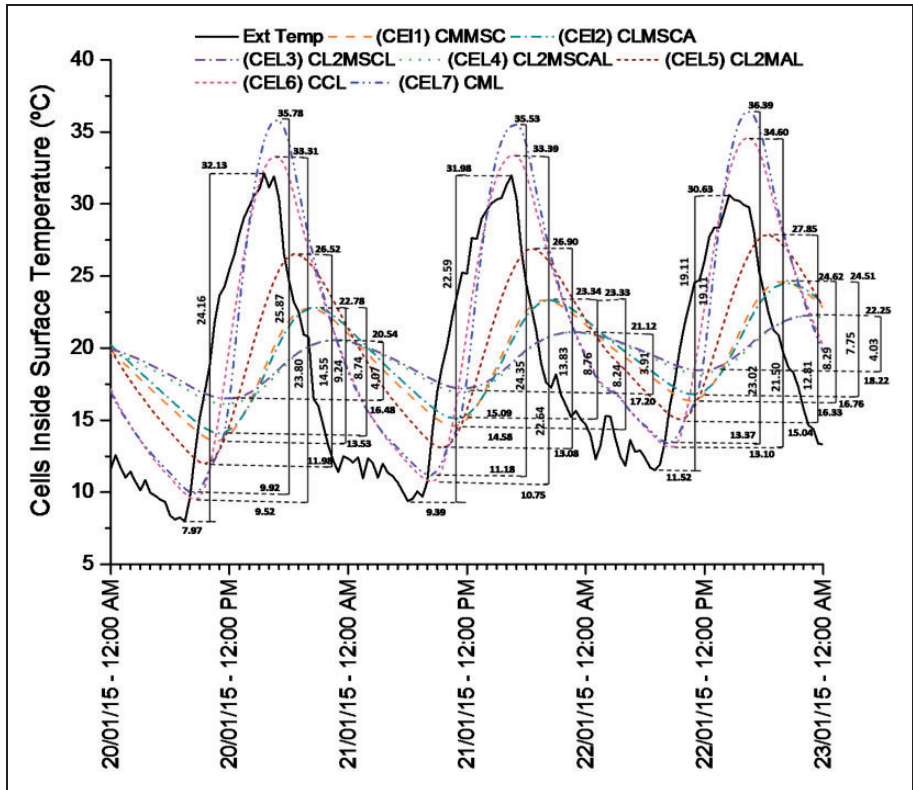


Figure 11. Inside surface temperatures of constructive components.

Figure 12 depicts average values of thermal amplitudes and decrement factor for constructive components under study tested in the experimental cells. It can be observed that cell 4 (CL2MSCAL = 0.166) and cell 3 (CL2MSCL = 0.181) provide the lowest decrement factor, formed by two plates of reinforced mortar filled with soil-cement and soil-cement-sawdust, respectively. These decrement factor results expressed as percentage of specimens tested respect to component CCL (100%) are as follows: CML (96.66%), CMMSC (60%), CL2MAL (55.55%), CLMSCA (35.55%), CL2MSCL (0.18%) and CL2MSCAL (0.17%).

Table 7 shows average and day by day thermal lag values determined from 20 to 23 January on constructive components under study. Figure 13 shows a comparative graph of thermal lag that goes in order of decreasing values as follows: CL2MSCAL = CL2MSCL > CLMSCA > CMMSC > CL2MAL > CML > CCL. This indicates that constructive components CL2MSCAL and CL2MSCL provide a higher thermal lag (7:37 h) than the rest of the components tested. This thermal lag value falls within the recommended standards suggested by several experts for extreme climates.³⁶ A detailed graph showing differences in thermal lag for each component is indicated

in Figure 14 for day 20 January, where the highest thermal lag 7:37 h was observed to present in components CL2MSCAL and CL2MSCL in both cases.

After analysing the thermal lag of the constructive components under study, CL2MSCL and CL2MSCAL specimens, the first soil filled and the second soil + sawdust filled, both show the highest thermal lag values and lowest decrement factor. Bioclimatic and passive design strategies indicate that for mild and cold climate, more than 8 h of time lag would be needed, as was achieved by CL2MSCL and CL2MSCAL components. The inclusion of sawdust as a filler did not show to contribute to increase the thermal lag any further but contributed to reducing the weight of the component, but in this paper that analysis was not included for the sake of brevity.

Equivalent thermal conductivity results of constructive components

The equivalent thermal conductivity of constructive components was measured and their thermal insulating potential to be used as component for house living was assessed. Table 8 shows the equivalent thermal conductivity results of the constructive components tested. CL2MSCAL was shown to have the lowest

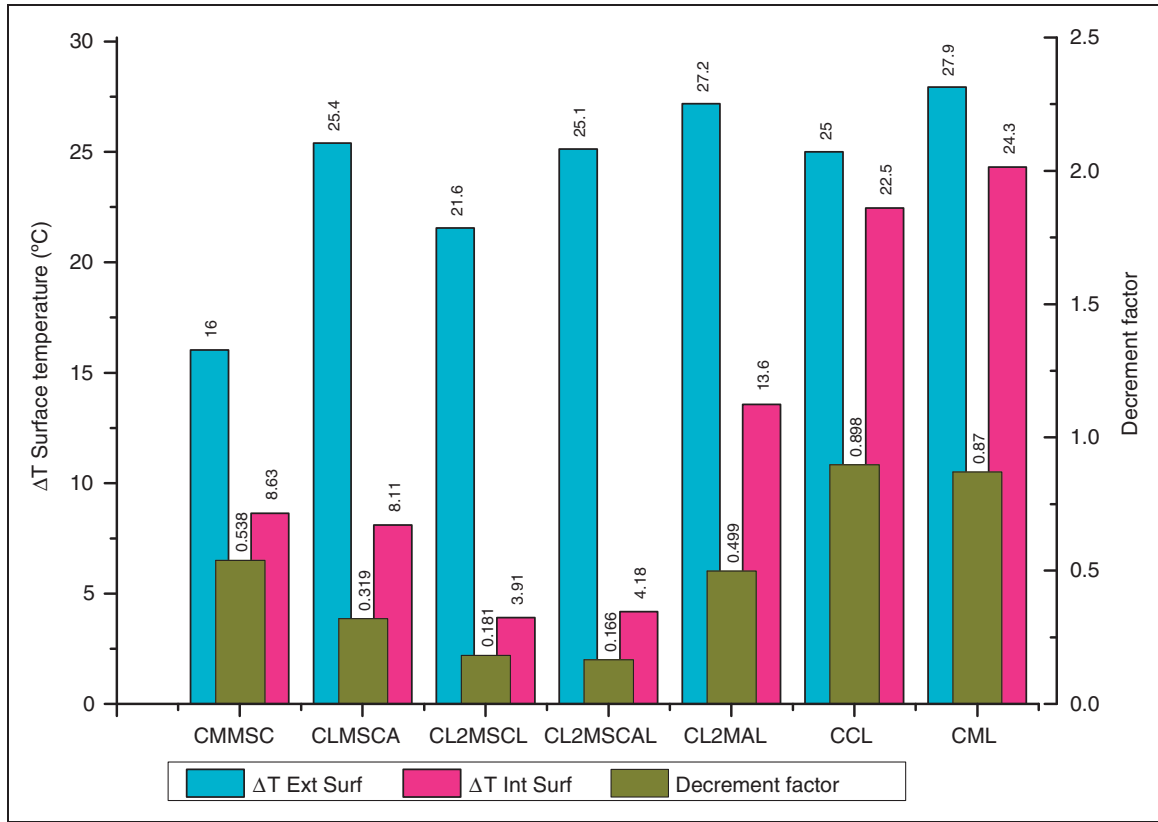


Figure 12. Average thermal amplitudes and decrement factor in components.

Table 7. Mean thermal time lag in constructive components.

Experimental cells	Day				Average thermal lag (h)
	20	21	22	23	
CML	1:30:00	1:00:00	1:00:00	1:00:00	1:07:00
CCL	1:00:00	1:00:00	1:00:00	1:00:00	1:00:00
CL2MAL	3:30:00	4:00:00	3:30:00	3:00:00	3:30:00
CL2MSCAL	7:00:00	8:00:00	7:30:00	8:00:00	7:37:30
CL2MSCL	7:00:00	8:00:00	7:30:00	8:00:00	7:37:30
CLMSCA	5:30:00	6:00:00	6:00:00	6:00:00	5:52:30
CMMSC	4:30:00	4:30:00	5:00:00	4:30:00	4:37:30

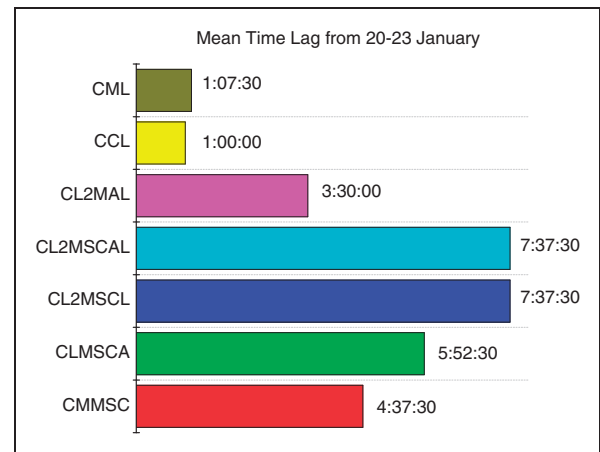


Figure 13. Mean thermal time lag of constructive components from 20 to 23 January.

equivalent thermal conductivity ($0.81 \text{ W}\cdot\text{m}^{-1}\cdot\text{K}^{-1}$) among the components tested and the highest equivalent thermal conductivity was shown for component CCL ($2.0 \text{ W}\cdot\text{m}^{-1}\cdot\text{K}^{-1}$) which was a slab of concrete plus finishing (annealed half red clay brick + mortar slurry) followed by CL2MAL ($1.86 \text{ W}\cdot\text{m}^{-1}\cdot\text{K}^{-1}$) whose configuration was similar to CL2MSCAL but was not filled.

Here the effect that the filler (soil + cement + sawdust) has on equivalent thermal conductivity was illustrated. Component CL2MSCL ($1.30 \text{ W}\cdot\text{m}^{-1}\cdot\text{K}^{-1}$) was similar to CL2MSCAL, but the filler did not contain sawdust that contributed to reducing the weight of the component (see density and equivalent thermal

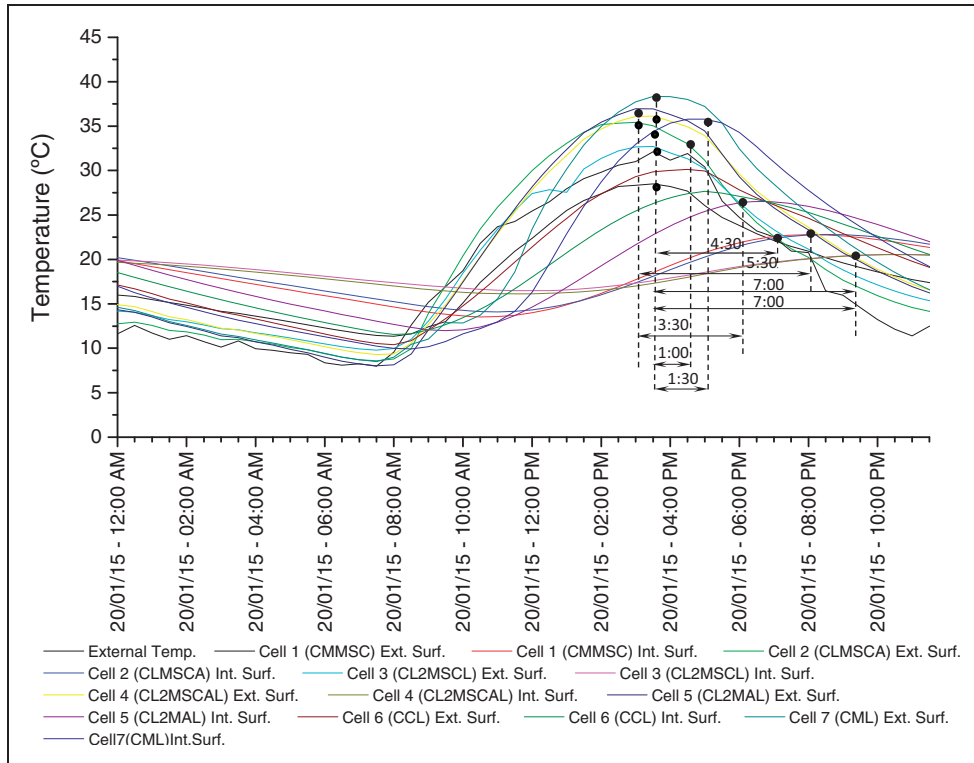


Figure 14. Thermal lag of constructive components for day January 20.

Table 8. Main thermal properties for each constructive component under study.

Part	λ	TC	$C \times 10^6$	Y	$\alpha \times 10^{-6}$	β	ρ	M_s	L	ΔT
CMMSC	1.60	8.01	0.547	8.01	0.584	2093.94	1896.9	379.38	0.200	12.4
CLMSCA	1.14	5.71	0.299	5.71	0.762	1308.41	1101.8	220.37	0.200	17.5
CL2MSCL	1.30	4.89	0.321	4.89	1.068	1252.78	1885.4	499.63	0.265	20.4
CL2MSCAL	0.81	3.07	0.196	3.07	1.098	776.60	1285.3	340.62	0.265	32.5
CL2MAL	1.86	7.03	0.379	7.03	1.298	1634.07	662.1	175.25	0.265	14.2
CCL	2.00	14.31	0.652	14.31	0.429	3055.35	2180.3	305.25	0.140	6.99
CML	1.05	16.18	0.582	16.18	0.117	3070.17	1850.0	120.25	0.065	6.18

Values of λ (equivalent thermal conductivity, $\text{W}\cdot\text{m}^{-1}\cdot\text{K}^{-1}$), TC (thermal conductance, $\text{W}\cdot\text{m}^{-2}\cdot\text{K}^{-1}$), C (heat capacity, $\text{J}\cdot\text{K}^{-1}$), Y (thermal admittance, $\text{W}\cdot\text{m}^{-2}\cdot\text{K}^{-1}$), α (diffusivity, $\text{m}^2\cdot\text{s}^{-1}$), β (effusivity, $\text{J}\cdot\text{m}^{-2}\cdot\text{K}^{-1}\cdot\text{s}^{-0.5}$), ρ (density, $\text{kg}\cdot\text{m}^{-3}$), M_s (mass density, $\text{kg}\cdot\text{m}^{-3}$), L (thickness, m) and ΔT (temperature difference, K).

conductivity of components^{6,56} and equivalent thermal conductivity. This contribution of sawdust was also observed in the equivalent thermal conductivity values comparing components CLMSCA ($1.14 \text{ W}\cdot\text{m}^{-1}\cdot\text{K}^{-1}$) – filler with sawdust, and CMMSC ($1.60 \text{ W}\cdot\text{m}^{-1}\cdot\text{K}^{-1}$) – filler without sawdust. CML component ($1.05 \text{ W}\cdot\text{m}^{-1}\cdot\text{K}^{-1}$) was shown to have almost half the equivalent thermal conductivity of CCL.

Other thermal properties of the constructive components tested, where determined from their experimentally obtained equivalent thermal conductivity and analytical

relationships^{6,56} such as thermal conductance (TC), heat capacity (C), thermal admittance (Y), diffusivity (α) and effusivity (β) are shown in Table 8. From Table 8, the CL2MSCAL was shown to exhibit the lowest values not only in decrement factor (0.166), equivalent thermal conductivity ($0.81 \text{ W}\cdot\text{m}^{-1}\cdot\text{K}^{-1}$) and density ($1285.38 \text{ kg}\cdot\text{m}^{-3}$) but also in TC ($3.07 \text{ W}\cdot\text{m}^{-2}\cdot\text{K}^{-1}$), heat capacity C ($0.196 \times 10^6 \text{ J}\cdot\text{K}^{-1}$), Y ($3.07 \text{ W}\cdot\text{m}^{-2}\cdot\text{K}^{-1}$), β ($776.6 \text{ J}\cdot\text{m}^{-2}\cdot\text{K}^{-1}\cdot\text{s}^{-0.5}$) and thermal diffusivity (α) ($1.098 \times 10^6 \text{ m}^2\cdot\text{s}^{-1}$), but highest values of thermal time lag (7:37 h) and temperature difference ΔT (32.55 K) from

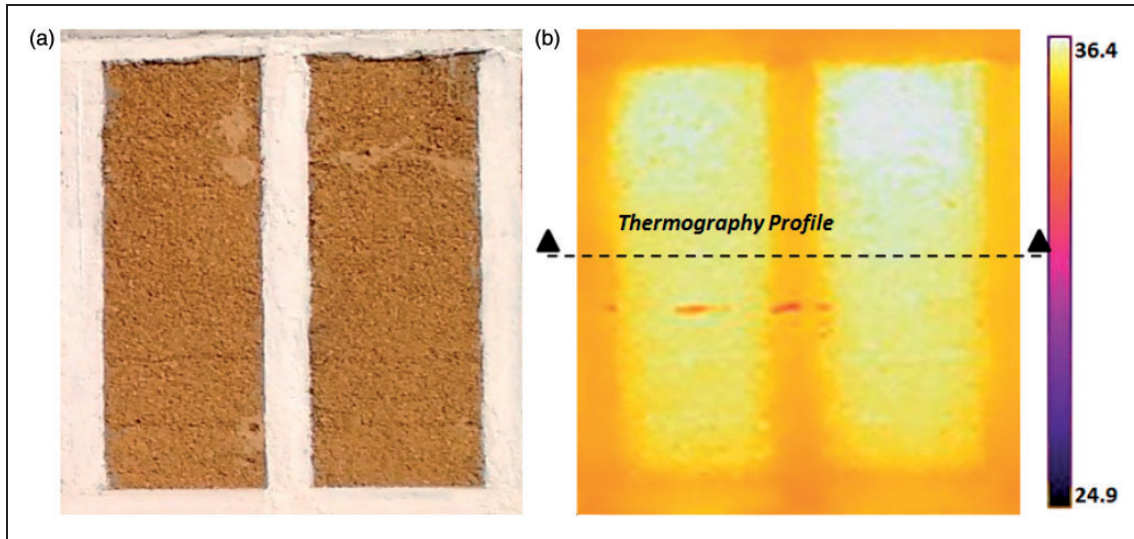


Figure 15. (a) Tested component and (b) thermal imaging of component taken on 21 June 2016 at 13:00 h.

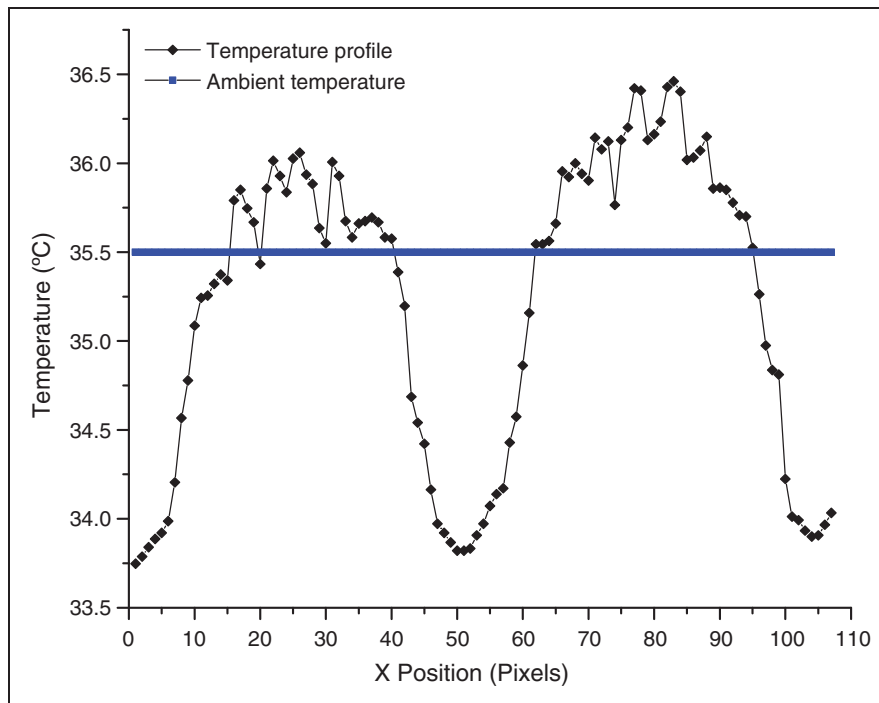


Figure 16. Temperature profile of component.

the components tested. Heat capacity represent the ability of a material to store heat while undergoing a given temperature change. Although this is not high, actually the opposite is true, in component CL2MSCAL, its thermal behaviour do not depend entirely of that parameter.

Thermal effusivity measures its ability to exchange heat with its surroundings and, in CL2MSCAL was very low and warm to the touch, and this has been suggested by Kinnane et al. ⁵⁶ that these types of

materials can improve thermal comfort. CL2MSCAL registered a low diffusivity that means it is a material that could prevent fast heat exchange with the environment. Thus, if thermal inertia² is understood in terms of thermal effusivity, a material with high thermal inertia (as is the case of CL2MSCAL) would not change its temperature as drastically as one with low thermal inertia (as is the case of CCL, β (3055.35 J·m⁻²·K⁻¹s^{-0.5}) or CML, β (3070.17 J·m⁻²·K⁻¹s^{-0.5})).

Thermal bridge effects of constructive components

Thermal bridge effects between the soil sawdust part and the reinforced concrete part were roughly studied performing a thermography measurement to determine the outside surface temperature on constructive component CLMSCA (reinforced concrete channels + soil–cement–sawdust). Figure 15(a) shows a picture of the constructive component CLMSCA where thermal measurements were carried out. Figure 15(b) shows a thermography image of the component taken at 13:00 h on 21 June 2016 with a FLIR T600 infrared camera that produces thermal images of 480×360 pixels of long wave. Figure 16 shows a 2D temperature profile from thermography image. This image indicates an irregular pattern of temperature values that fluctuate between 33.9°C and 36.3°C .

Temperature was reduced about 2.4°C when the profile line reached the reinforced concrete; which was caused by the difference in thermal conductivity of soil and reinforced concrete. However, because channels' thickness was small, a notorious temperature difference was not presented. Of course that does not mean that the thermal bridge effect is negligible, but for a constructive system of walls or slabs it could be suggested that junction between soil and reinforced concrete be at a larger distance to reduce thermal energy losses.

Conclusions

Seven experimental chambers were built to measure the thermal lag and decrement factor of hybrid constructive components CCL, CML, CMMSC, CLMSCA, CL2MSCL, CL2MSCAL and CL2MAL. Best results were found for component CL2MSCAL (formed by two reinforced concrete channels filled with soil–cement–sawdust and a slab of reinforced concrete-half red clay brick–cement–sand mortar slurry as finishing) that has a thermal conductivity of $0.81 \text{ W}\cdot\text{m}^{-1}\cdot\text{K}^{-1}$, a thermal damping of 81.5% (decrement factor of 0.166) and time lag of 7:37 h compared to CCL (traditional concrete slabs) that present a time lag of 1 h and decrement factor of 0.9. Component CL2MSCAL performed better than the rest of the components also.

Much has been said about the thermal conductivity or thermal mass of soil, but at present there are no similar experimental studies on large building components reported in the literature. In this study, the experiments were conducted on real-scale samples and using thermal chambers (prototypes) built for this purpose. The values of thermal lag and decrement factor in this study are important to achieve thermal comfort in semi-cold and cold conditions where thermal

oscillations are above 14°C since a high thermal resistance insulating material does not ensure a good thermal performance, even more in climates with high thermal oscillations. Under such conditions, the construction envelope of buildings must have a high thermal storage. The results observed in this study are important when the aim is to minimize electric energy consumption since it limits heat flow at peak hours where temperatures reach the highest values. Such components can provide an ecologic alternative for energy saving and thermal comfort.

Authors' contribution

All authors contributed equally in the preparation of this manuscript.

Declaration of conflicting interests

The author(s) declared no potential conflicts of interest with respect to the research, authorship, and/or publication of this article.

Funding

The author(s) disclosed receipt of the following financial support for the research, authorship, and/or publication of this article: This study received the financial support from National Council for Science and Technology (Conav-Conacyt) under Project No. 2013-01-206387 and Instituto Politecnico Nacional (Project No. SIP 2014/RE/110 and Project No. SIP: 20151304).

References

1. Maalouf C, Le ADT, Umurigirwa SB, Lachi M and Douzane O. Study of hygrothermal behaviour of a hemp concrete building envelope under summer conditions in France. *Energy Build* 2014; 77: 48–57.
2. Maas JVD and Maldonado E. A new thermal inertia model based on effusivity. *Int J Sol Energy* 1997; 19: 131–160.
3. Pavlović SS, Stanković SB, Popović DM and Poparić GB. Transient thermal response of textile fabrics made of natural and regenerated cellulose fibers. *Polym Test* 2014; 34: 97–102.
4. Faye M, Lartigue B and Sambou V. A new procedure for the experimental measurement of the effective heat capacity of wall elements. *Energy Build* 2015; 103: 62–69.
5. Maillot D, André S, Batsale JC, Degiovanni A and Moyne C. *Thermal quadrupoles*. New York: Wiley, 2000.
6. CIBSE Guide A3. *Thermal properties of building structures*. Appendix 3.A6. London: CIBSE, 2006.
7. Fatiha YE, Nacer M, Abd-El-Hamid A and Sauvageot H. Temperature variations in a housing of the semi-arid region of Djelfa (Algeria). *Build Environ* 2003; 38: 511–519.
8. Aroni S. On energy conservation characteristics of autoclaved aerated concrete. *Mater Struct* 1990; 23: 68–77.
9. Orasa JA and Carpentier T. Thermal inertia effect in old buildings. *Eur J Sci Res* 2009; 27: 228–233.
10. Roucoult JM, Douzane O and Langlet T. Incorporation of thermal inertia in the aim of installing a natural night time ventilation system in buildings. *Energy Build* 1999; 29: 129–133.
11. Kontoleon KJ and Eumorfopoulou EA. The influence of wall orientation and exterior surface solar absorptivity on time lag

- and decrement factor in the Greek region. *Renew Energ* 2008; 33: 1652–1664.
12. Ulgen K. Experimental and theoretical investigation of effects of wall's thermophysical properties on time lag and decrement factor. *Energy Build* 2002; 34: 273–278.
 13. Tsilingiris PT. The influence of heat capacity and its spatial distribution on the transient wall thermal behavior under the effect of harmonically time-varying driving forces. *Build Environ* 2006; 41: 590–601.
 14. Asan H. Effects of wall's insulation thickness and position on time lag and decrement factor. *Energy Build* 1998; 28: 299–305.
 15. Vecchia F. Clima y ambiente construido: a abordagem dinâmica aplicada ao conforto humano. PhD Thesis. Universidade de São Paulo (USP), Departamento de Geografia, Faculdade de Filosofia, Letras e Ciências Humanas (FFLCH), São Paulo, Brasil; 1997 [in Portuguese].
 16. ASTM D2487-11. *Standard practice for classification of soils for engineering purposes (unified soil classification system)*. West Conshohocken, PA: ASTM International, 2011. DOI: 10.1520/D2487-11.
 17. Krüger EL, Adriazola M, Matoski A and Iwakiri S. Thermal analysis of wood-cement panel: Heat flux and indoor temperature measurements in test cells. *Constr Build Mater* 2009; 23: 2299–2305.
 18. Bederina M, Marmoret L and Mezreb K. Effect of the addition of wood shavings on thermal conductivity of sand concretes: Experimental study and modeling. *Constr Build Mater* 2007; 21: 662–668.
 19. Morris F, Ahmed AZ and Zakaria NZ. Thermal performance of naturally ventilated test building with pitch and ceiling insulation. In *Proceedings of 3rd international symposium & exhibition in sustainable energy & environment (ISESEE)*, 1–3 June 2011, pp.221–226. Malacca, Malaysia: IEEE. DOI: 10.1109/ISESEE.2011.5977093.
 20. Ouldoukhitine SE, Belarbi R, Jaffal I and Trabelsi A. Assessment of green roof thermal behavior: A coupled heat and mass transfer model. *Build Environ* 2011; 46: 2624–2631.
 21. Tibério-Cardoso G, Claro-Neto S and Vecchia F. Rigid foam polyurethane (PU) derived from castor oil (*Ricinus communis*) for thermal insulation in roof systems. *J Foar* 2012; 348–356.
 22. Gameros-González G. Agua encapsulada como amortiguador térmico sobre losas de concreto. MSc Thesis, Universidad de Colima, Faculty of Architecture and Design, Colima, Mexico, 2007.
 23. Roels S and Deurincq M. The effect of a reflective underlay on the global thermal behavior of pitched roof. *Build Environ* 2011; 46: 134–143.
 24. Shea A, Lawrence M and Walker P. Hygrothermal performance of an experimental hemp-lime building. *Constr Build Mater* 2012; 36: 270–275.
 25. Vecchia F and Castañeda N. Evaluación del comportamiento térmico de casa experimental con bajareque mejorado. In: *Proceedings of ENCAC-ELACAC 2005*, Halagaos Brazil, October 5–7 2005, pp.2156–2163.
 26. Vecchia F and Castañeda N. Reacción ante el calor de cuatro sistemas de cubiertas. *Ingeniería Revista Académica, Universidad Autónoma de Yucatán* 2006; 10: 17–23.
 27. Singh MK, Mahapatra S, Atreya SK and Givoni B. Thermal monitoring and indoor temperature modeling in vernacular buildings of North-East India. *Energy Build* 2010; 42: 1610–1618.
 28. Roma Jr LC, Martello LS and Savastano Jr H. Evaluation of mechanical, physical and thermal performance of cement-based tiles reinforced with vegetable fibers. *Constr Build Mater* 2008; 22: 668–674.
 29. Teemusk A and Mander U. Temperature regime of planted roofs compared with conventional roofing systems. *Ecol Eng* 2010; 36: 91–95.
 30. Alavéz-Ramírez R, Chiñas-Castillo F, Morales-Dominguez VJ and Ortiz-Guzman M. Thermal conductivity of coconut fibre filled ferrocement sandwich panels. *Constr Build Mater* 2012; 37: 425–431.
 31. Alavéz-Ramírez R, Chiñas-Castillo F, Morales-Dominguez VJ and Ortiz-Guzman M. Thermal lag and decrement factor of a coconut-ferrocement roofing system. *Constr Build Mater* 2014; 55: 246–256.
 32. INEGI *Censo de Población y Vivienda 2000 y 2010*. Instituto Nacional de Geografía y Estadística, <http://www.inegi.org.mx/est/contenidos/proyectos/ccpv/cpv2010/Default.aspx> (2010, accessed 15 October 2016).
 33. INEGI *Censo de Población y Vivienda 1970 a 2010*. Instituto Nacional de Geografía y Estadística, <http://www.inegi.org.mx/est/contenidos/proyectos/ccpv/cpv2010/Default.aspx> <http://www.inegi.org.mx/est/contenidos/proyectos/ccpv/cpv2010/Default.aspx> (2010, accessed 15 October 2016).
 34. Cabahug R and Robles-Austriaco L. Ferrocement-construction material for urban housing. *J Ferrocement* 1998; 28: 41–46.
 35. Wainshtok-Rivas H. Low-cost housing built with ferrocement precast elements. *J Ferrocement* 1994; 24: 29–34.
 36. Fuentes-Freixanet VA. *Mapas bioclimáticos de la república mexicana*. México: Editorial UAM (División CyAD, Azcapotzalco), 2014.
 37. Köppen W. *Climatología con un estudio de los climas de la tierra*. Direct version from Hendrichs Pérez Pedro R. México: Fondo de Cultura Económica, 1948.
 38. SMN. *Normales climatológicas*. México, D.F: DGGM. Servicio Meteorológico Nacional, 1976.
 39. García E. *Modificaciones al Sistema de Clasificación Climática de Köppen (para adaptarlo a las condiciones de la República Mexicana)*. México, D.F: Offset Larios S.A, 1988.
 40. Koenigsberger OH. *Viviendas y edificios en zonas cálidas y tropicales*. Madrid, España: Editorial Paraninfo, 1977.
 41. Szokolay SV. *Passive and low energy design for thermal and visual comfort*. PLEA'84 México, vol. 1, New York, USA: Pergamon Press, 1984.
 42. ASTM C150/C150M-16e1. *Standard specification for Portland cement*. West Conshohocken, PA: ASTM International, 2016. DOI: 10.1520/C0150_C0150M-16E01.
 43. Ramírez-Arellanes S. Determinación del módulo de elasticidad y la relación de Poisson del mortero cemento-arena para la ciudad de Oaxaca y área conurbada. BSc Thesis, Instituto Tecnológico de Oaxaca, 2006.
 44. ASTM C39/C39M-16b. *Standard test method for compressive strength of cylindrical concrete specimens*. West Conshohocken, PA: ASTM International, 2016. DOI: 10.1520/C0039_C0039M-16B.
 45. ASTM C109/C109M-16a. *Standard test method for compressive strength of hydraulic cement mortars (using 2-in. or [50-mm] cube specimens)*. West Conshohocken, PA: ASTM International, 2016. DOI: 10.1520/C0109_C0109M-16A.
 46. ASTM C469/C469M-14. *Standard test method for static modulus of elasticity and poisson's ratio of concrete in compression*. West Conshohocken, PA: ASTM International, 2014. DOI: 10.1520/C0469_C0469M.
 47. Casagrande A. Classification and identification of soils. *Am Soc Civil Eng* 1948; 113: 901–930.
 48. NMX-AA-061-1985. *Protección al ambiente-contaminación del suelo-residuos sólidos municipales-determinación de la generación*. México, México: Secretaria de Comercio y Fomento Industrial, Dirección General de Normas, 1985, pp.3–16.
 49. ASTM D422-63(2007)e2. *Standard test method for particle-size analysis of soils (withdrawn 2016)*. West Conshohocken, PA: ASTM International, 2007. DOI: 10.1520/D0422-63R07E02.

50. AASHTO T99. *Standard method of test for the moisture-density relations of soils*. Washington, DC: American Association of State Highway & Transportation Officials, 1990.
51. Bahar R, Benazzoug M and Kenai S. Performance of compacted cement-stabilized soil. *Cem Concr Compos* 2004; 26: 811–820.
52. Roseto O. Bloques con Mezclas Hipercomprimidas de Suelo-Cemento. *Revista Cemento* 1996; 2: 11–13.
53. NMX-C-037-ONNCCE-2005. *Industria de la construccion-mamposteria-determinacion de la absorcion total y la absorcion inicial de agua en bloques, tabiques o ladrillos y tabicones-metodo de ensayo*. Organismo Nacional de Normalización y Certificación de la Construcción y Edificación S.C. (ONNCCE), México, 2005.
54. Haik Y, Shahin TM and Sivaloganathan S. *Engineering design process*. 2nd ed. USA: Cengage Learning, 2010.
55. ASTM C177-13. *Standard test method for steady state heat flux measurements and thermal transmission properties by means of the guarded hot-plate apparatus*. West Conshohocken, PA: ASTM International, 2013. DOI: 10.1520/C0177.
56. Kinnane O, McGranaghan G, Walker R, Pavia S, Byrne G and Robinson A. Experimental investigation of thermal inertia properties in hemp-lime concrete walls. In: *Proceedings of the 10th conference on advanced building skins*. Bern, Switzerland: Economic Forum, 3–4 November 2015, pp.942–949.